

# First characterization of chemical environments using energy dispersive inelastic x-ray scattering induced by an x-ray tube

Cite as: Rev. Sci. Instrum. **92**, 013102 (2021); <https://doi.org/10.1063/5.0026061>

Submitted: 20 August 2020 . Accepted: 12 December 2020 . Published Online: 05 January 2021

 Roberto Daniel Pérez, Juan José Leani,  José Ignacio Robledo, and Héctor Jorge Sánchez



View Online



Export Citation



CrossMark

## ARTICLES YOU MAY BE INTERESTED IN

[First result of photoabsorption spectroscopic studies beamline \(PASS, BL-07\) installed on Indus-1 synchrotron source](#)




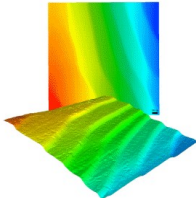
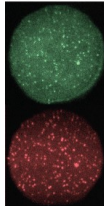
Review of Scientific Instruments **92**, 015106 (2021); <https://doi.org/10.1063/5.0020222>

[An experimental setup for dip-coating of thin films for organic solar cells under microgravity conditions](#)

Review of Scientific Instruments **92**, 015108 (2021); <https://doi.org/10.1063/5.0018223>

[Systematic calibration method based on acceleration and angular rate measurements for fiber-optic gyro SINS](#)

Review of Scientific Instruments **92**, 015001 (2021); <https://doi.org/10.1063/5.0023674>

	<p>Nanopositioning Systems</p> 	<p>Modular Motion Control</p> 	<p>AFM and NSOM Instruments</p> 	<p>Single Molecule Microscopes</p> 
---	--	--	---	--

# First characterization of chemical environments using energy dispersive inelastic x-ray scattering induced by an x-ray tube

Cite as: Rev. Sci. Instrum. 92, 013102 (2021); doi: 10.1063/5.0026061

Submitted: 20 August 2020 • Accepted: 12 December 2020 •

Published Online: 5 January 2021



View Online



Export Citation



CrossMark

Roberto Daniel Pérez,<sup>a)</sup>  Juan José Leani, José Ignacio Robledo,  and Héctor Jorge Sánchez

## AFFILIATIONS

IFEG, National Scientific and Technical Research Council (CONICET), X5000HUA Córdoba, Argentina and FaMAF, Universidad Nacional de Córdoba (UNC), X5000HUA Córdoba, Argentina

<sup>a)</sup> Author to whom correspondence should be addressed: [danperez@famaf.unc.edu.ar](mailto:danperez@famaf.unc.edu.ar)

## ABSTRACT

Energy Dispersive Inelastic X-ray Scattering (EDIXS) is a reliable technique for the discrimination and characterization of local chemical environments. By means of this methodology, the speciation of samples has been attained in a variety of samples and experimental conditions, such as total reflection, grazing incidence, and confocal setups. Until now, due to the requirement of a monochromatic and intense exciting beam, this tool had been applied using exclusively synchrotron radiation sources. We present, for the first time, results of test measurements using EDIXS for chemical characterization implemented in a conventional x-ray tube based laboratory. The results show good discrimination between different iron compounds under study, suggesting the real possibility of routine chemical state characterizations of samples by means of EDIXS using a conventional x-ray tube.

Published under license by AIP Publishing. <https://doi.org/10.1063/5.0026061>

## I. INTRODUCTION

Energy Dispersive Inelastic X-ray Scattering (EDIXS) refers to a spectrometric technique that makes use of the intrinsic properties of the atomic processes at the core level involving photons (see, for example, Ref. 1, for an updated EDIXS review). This is the case of Resonant Inelastic X-ray Scattering (RIXS),<sup>2–9</sup> also named X-ray Resonant Raman Scattering (RRS), which, in combination with the experimental advantages of an energy dispersive setup (EDS), allows for obtaining the discrimination of chemical environments in diverse samples and experimental conditions. As a drawback, the spectral differences between the species will become smaller as a consequence of the low spectral resolving power of the EDS, which requires the implementation of a more sophisticated spectral evaluation.

During the last few years, several works have shown applications of this EDIXS tool in a variety of irradiation geometries and samples of interest, obtaining in this way different kinds of information from the studied materials. The classic 45°–45° configuration for sample bulk examinations,<sup>10–12</sup> total reflection geometry for inspecting material surfaces and samples on reflectors,<sup>13,14</sup>

grazing incidence setups for depth-resolved analysis,<sup>15–17</sup> and confocal geometry are used for obtaining chemical speciation in a 3D regime,<sup>18</sup> reaching micro- and even nano-metric resolutions. Clearly, EDIXS can be applied in a variety of areas of both science and technology, such as chemistry, biology, environment, cultural heritage, and materials science.

Since an essential requirement for the application of the EDIXS methodology is an exciting monochromatic beam having energy below but close to the K-absorption edge of an element of interest, this technique has been applied until now only in synchrotron radiation facilities, making use of the advantage of the easy tunable beam and the availability of high photon fluxes.

This work presents results of first test measurements of EDIXS using a conventional x-ray tube as the source, for chemical state discrimination of metal samples.

The measurements were carried out at the non-conventional X-Ray Fluorescence (XRF) techniques laboratory of the atomic and nuclear spectroscopy group at the National University of Córdoba (UNC), Argentina. The preliminary setup employed for this experience was very simple and mainly composed by using an x-ray tube (with a Mo anode), a Si(111) crystal (used as a monochromator),

a couple of slits, a versatile sample holder, and a Si-pin diode x-ray detector.

The studied samples were three pure compounds of iron:  $\text{Fe}_2\text{O}_3$ ,  $\text{Fe}_3\text{O}_4$ , and a carbon steel. Several RIXS spectra of each sample were acquired using an incident beam energy below the Fe-K edge. RIXS peaks were then analyzed by a multivariate method [Principal Component Analysis (PCA)] in order to properly discriminate the fine structure of each spectrum.

The results show that the fine structure of each RIXS peak clearly depends on the studied sample, i.e., the chemical state of iron. This outcome opens the possibility of local environment characterizations by means of RIXS using a simple energy dispersive setup combined with a conventional x-ray tube.

This promising application of EDIXS where synchrotron radiation is not needed allows for the study of chemical states in different kinds of samples at a local x-ray tube based laboratory; characterization nowadays is difficult, or even impossible, to achieve by conventional methods.

## II. EXPERIMENTAL

### A. Design of the spectrometer

The first experiment proposed for the spectrometer was the analysis of the local chemical environment of iron composites by EDIXS. To accomplish this goal, a monochromatic beam with an energy near (but below) the K-absorption edge of iron (7.11 keV) had to be employed. For a conventional laboratory, the access to such an excitation beam represents a challenging task since the monochromatization of an x-ray source drastically reduces the available photon flux. This effect is clearly observed when a crystal monochromator is attached to an x-ray tube to extract photons of well-defined energy from the continuous part of the spectrum. This setup is frequently used in conventional laboratories since it represents a low cost and simple solution for the issue. Preliminary studies in our laboratory with a crystal monochromator show that this simple setup must be improved in some way in order to obtain a practical photon rate for the resonant inelastic x-ray scattering of any element. An efficient strategy to fulfill this goal is to increase the incident photon flux over the crystal with energies around the absorption edge of iron, which has already been developed using different setups.<sup>9,19,20</sup> We implemented this strategy by adding a Beam Guide (BG)<sup>21</sup> made of two parallel highly polished plates, which probably is the simplest one. It was attached at the output of the x-ray tube to produce a quasi-parallel beam toward the crystal. Inside the gaps, photons are transmitted by total reflection with higher efficiency for low energy photons.

Finally, it is interesting to compare the number of photons transmitted by the BG with a simple double slit collimator with equivalent dimensions (i.e., 0.5 mm slit aperture, 10 mm wide, and 60 mm distance between slits). To simplify the calculations, it is convenient to consider the x-ray tube as a collection of point sources covering the extension of the anode. For any one of these points, the difference between both devices lies in the solid angle subtended from the position of the source. In both cases, it can be written as  $\Delta\Omega = \Delta\theta \times \Delta\phi$ , where  $\Delta\theta$  is the angular aperture in the vertical plane and  $\Delta\phi$  in the plane of the steel foils. For the double slit collimator,  $\Delta\theta = 2.27$  mrad, while for the BG, it is increased to 5 mrad by the

contribution of x-ray total reflection. It means that the photon flux for a point source can be improved approximately by a factor of two by the BG. It is still valid for an extended source as an x-ray tube considering it as a composition of point sources.

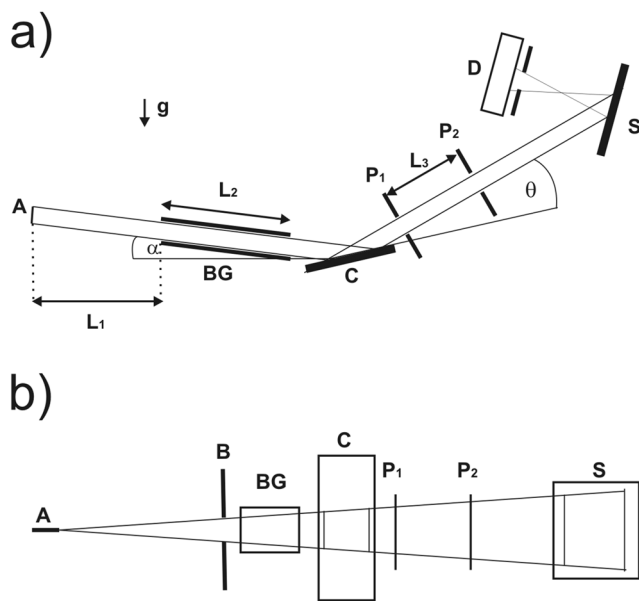
### B. Instrumentation

The measurements were performed at the non-conventional XRF techniques laboratory of the atomic and nuclear spectroscopy group at the National University of Córdoba, Argentina. For this experiment a dedicated spectrometer with a tunable monochromatic excitation was developed.

The instrument employs a flat crystal Si(111) combined with a BG made of highly polished stained steel foils to select the desirable wavelength from the continuous polychromatic spectrum induced by using a conventional x-ray diffraction tube. The angular position of the crystal was adjusted by means of a commercial high precision goniometer. A versatile sample holder keeps the sample in a reproducible position, and its x-ray emission was registered with a Si-pin diode x-ray detector AMPTEK-XR100T (180 eV @ Mn-K $\alpha$  line). In the following, a detailed description of the different components of the experimental setup is presented.

The x-ray source was a Mo x-ray diffraction tube Philips model PW2275/20 with a focus dimension of  $0.4 \times 12$  mm<sup>2</sup> (long fine focus) and its symmetry axis on the vertical direction. The selected output shutter was the focus line, with an effective emission area of  $0.04 \times 12.6$  mm<sup>2</sup> pointed down at  $6^\circ$  with respect to the horizontal plane. To obtain a quasi-parallel beam at this direction with high spectral brightness, a beam guide made of two parallel, highly polished, stained steel foils was carefully aligned using manual positioners (see Fig. 1). The dimensions of the foils were  $60 \times 12$  mm<sup>2</sup> and the separation gap was 0.5 mm.

According to the spectrometer design previously described, a crystal monochromator is required as to efficiently select wavelength photons of  $\sim 7.050$  keV (1.7557 Å). Between all possible crystals able to select this wavelength, silicon was chosen because it is a multi-purpose crystal with good reflectivity and excellent wavelength resolution, which nowadays has a low cost. In addition, silicon crystals are of easy access due to a high demand from the semiconductor industry. From all possible orientations, we chose Si(111) with an interplanar distance between atomic planes of 3.135 Å in order to minimize Bragg reflection of higher orders than the first one. This condition is fulfilled by the Si(111) since all even Bragg reflections are forbidden. In addition, the third Bragg reflection, which is the first non-forbidden reflection, has considerably lower intensity than the first order one. The third Bragg reflection selects photons of 21.171 keV (0.5852 Å) from an energy region of the Mo x-ray tube spectrum with a low flux rate that has a low background contribution. In addition, the form factor for the coherent dispersion on silicon is reduced almost by a factor of two at the momentum transfer of the third Bragg reflection. Despite all these factors, the third Bragg reflection is still present in the output of the crystal monochromator and must be taken into account for a RIXS analysis. The second non-forbidden reflection is the fifth order one, which occurs at 35.285 keV (0.3511 Å). In order to suppress this reflection, and also reduce the third order reflection, the x-ray tube was set at 35 kV–20 mA.



**FIG. 1.** Schematic diagram of the spectrometer where the beam path is traced: (a) is the side view and (b) is the top view. In both figures A is the Mo anode of the x-ray tube, BG is the input beam guide, P1 and P2 are two slits of 0.5 mm, C is the Si(111) crystal, S is the sample, D is the XR100T Amptek x-ray detector,  $\alpha = 6^\circ$  is the angle of the primary beam with the horizontal,  $\theta = 16.26^\circ$  is the reflected angle of the Bragg diffraction and B is a circular collimator of 3 mm of diameter disposed at the entrance of the optical device at 2 cm from S. In the bottom of the Figure (a) the distances L1, L2 and L3 are 50 mm, 60 mm, and 40 mm, respectively.

The Si(111) requires an incident angle of  $16.26^\circ$  to select the 7.050 keV photons. This angle was manually set using a Newport high precision rotation stage (model RS40), with an angular resolution of  $0.2^\circ$ . The Si(111) was analyzed by conventional x-ray diffraction to corroborate its crystalline structure. The measured  $d$  spacing of the Si(111) atomic planes was  $3.135 \text{ \AA}$  with a relative variation of  $\Delta d/d = 9.3 \times 10^{-3}$ . A simple calculation considering the cross section of the incident beam (0.5 mm) and the Bragg incident angle ( $16.26^\circ$ ) shows that the length of the crystal must be at least 1.8 mm. Therefore, we used a  $10 \times 20 \text{ mm}^2$  highly polished Si(111) crystal of 0.5 mm thickness placed as shown in Fig. 1. Attenuation calculations show that the Si penetration depth for x-ray photons of 7.050 keV, with an incident angle of  $16.26^\circ$ , is only of 0.027 mm, which demonstrates that the thickness of the crystal employed is thick enough to reflect more than 90% of the monochromatic beam.

Two pairs of 0.5 mm slits were placed as shown in Fig. 1 in order to select the reflected beam. They were separated by 40 mm, and the first slit was set at 20 mm from the center of the Si(111) crystal. After passing through the slits, the beam was incident on the sample. The detector was placed normal to the sample, and the angle subtended between the incident and the detected beam was  $80^\circ$ . A 3 mm, the lead collimator was set in front of the x-ray detector, and the sample–detector distance was 20 mm. The measured FWHM of the monochromatic line was  $70 \pm 5 \text{ eV}$ . We registered in transmission geometry the scattering radiation from a PE plastic film (0.1 mm thickness) at a low angle ( $10^\circ$ ) with the Si pin

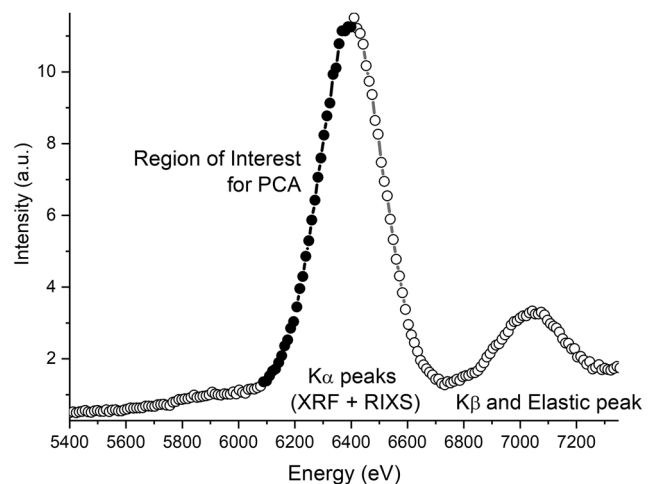
detector AMPTEK XR100T. In this setup, the coherent scattering dominates, so we had no Compton shift in the scattering peak. Thus, the FWHM of this peak is  $\Delta E_{\text{peak}}^2 = \Delta E_{\text{det}}^2 + \Delta E^2$ . Here,  $\Delta E_{\text{det}}$  is the energy resolution of the detector at 7050 eV and  $\Delta E$  is the energy resolution of the monochromator. The energy resolution of the detector was previously determined with two radioactive sources: Fe55 and Am241. For our spectrometer,  $\Delta E_{\text{peak}} = 258 \text{ eV}$  and  $\Delta E_{\text{det}} = 248 \text{ eV}$ .

### C. Samples and measurements

The studied samples consisted of three compounds of iron: a standard carbon steel, a Fe(III) sample ( $\text{Fe}_2\text{O}_3 + 25\%$  of cellulose), and a Fe(II, III) ( $\text{Fe}_3\text{O}_4$ ) pure oxide. The first compound was in the solid state with a polished surface ready to be analyzed. Conversely, the iron oxides were in powder forms that were prepared as pressed pellets using a hydraulic press set at 5 ton. Cylindrical pellets of 15 mm diameter and 1 mm thickness were obtained. The samples were placed with a fixed sample holder previously aligned to the center of the monochromatic beam path using ontological radiographies. The beam impinged the sample over an extended area with a  $10^\circ$  incident angle reducing sample inhomogeneity effects on RIXS emission. The output angle was  $90^\circ$  obtained by placing the detector perpendicular to the sample.

Five RIXS spectra of each sample were acquired using an incident beam energy centered on 7050 eV (i.e., below the Fe–K edge). RIXS peaks were analyzed by Principal Component Analysis (PCA) in order to properly discriminate the fine structure of each spectrum.

The acquisition live-time was 3 h/spectrum, and the measurements were carried out in air atmosphere. A mean value of 35 cps was observed in the RIXS peaks of the analyzed samples. Figure 2 shows an example of a spectrum acquired from the  $\text{Fe}_2\text{O}_3$  sample. The region of interest for the PCA analysis is also indicated.



**FIG. 2.** Example of a spectrum acquired from a  $\text{Fe}_2\text{O}_3$  sample. XRF and RIXS peaks are shown as well as the elastic peak. Region of interest for the analysis also indicated. Incident Energy of 7050 eV (i.e., below the Fe–K edge).

#### D. Preprocessing of spectra and data analysis

As to be able to analyze the measured spectra, a first small preprocessing step was needed. Only the region of the low energy tail of the RIXS peak was considered for this analysis. All the spectra were normalized to the value of the maximum amplitude of each RIXS peak as to remove any intensity fluctuation (due to sample scattering and incident flux fluctuations, among others), which is considered as undesired variability. This is one possible way of effectively enhancing the contribution of the RIXS oscillations to the total variability of the spectrum. The multivariate statistical analysis tool that was used for the analysis once the dataset was preprocessed is known as principal component analysis.<sup>22</sup> It is an exploratory methodology that allows us to study the variance–covariance structure of a given dataset. This technique has been repeatedly used in x-ray spectroscopy due to its versatility and simplicity in application and interpretation.<sup>16,23,24</sup> This methodology obtains a specific set of vectors, called the Principal Components (PCs), which are orthogonal to each other and, therefore, explain a different proportion of the variance in the dataset.<sup>22</sup> By doing so, one may study the spectra scores in the different components and study the total variance by parts, in smaller fractions. In this way, it is possible to reduce the dimensionality of the dataset and simplify the extraction of information from it. It is important to understand that the principal components are ordered in decreasing amount of explained variance. Therefore, Principal Component 1 is the PC that explains the highest percentage of the total variability, Principal Component 2 is the second one, and so on. As to better comprehend this technique, the reader may refer to Ref. 22.

As mentioned before, a total of 15 spectra were measured, corresponding to five spectra measured from three different samples. The region of analysis for the PCA consisted in 32 energy channels, ranging in energies from 6024.19 eV to 6356 eV, 75 eV. Therefore, a  $15 \times 32$  matrix was used for the PCA procedure. Afterward, the resulting projections of the spectra on Principal Components 1–3 were studied.

#### E. Theoretical calculations

A proper measurement of a RIXS spectrum using the EDIXS technique requires being as close as possible to the absorption edge of the element of interest. As the resolution of the monochromator is rather low (70 eV), tuning the incident energy close to the edge will lead to a photoelectric effect and the appearance of characteristic fluorescent lines (particularly K $\alpha$  lines). In this situation, the width of the fluorescent line, due to the intrinsic FWHM of the detector, will overlap the RIXS peak with the low energy side of the K $\alpha$  lines. For this reason, before carrying out the experimental measurements, some theoretical calculations were performed in order to investigate the feasibility of discriminating the atomic environment via the RIXS signal.

The basic model of Shiraiwa and Fujino<sup>25</sup> for photon transport inside the sample, in combination with the Kramers–Heisenberg formulation<sup>26</sup> for the resonant inelastic interaction, was used to calculate the intensities of the different atomic processes involved. Specific information about the calculation procedure, the formulation employed, fundamental parameters, and coding can be seen in detail in the work of Sánchez *et al.*<sup>27</sup>

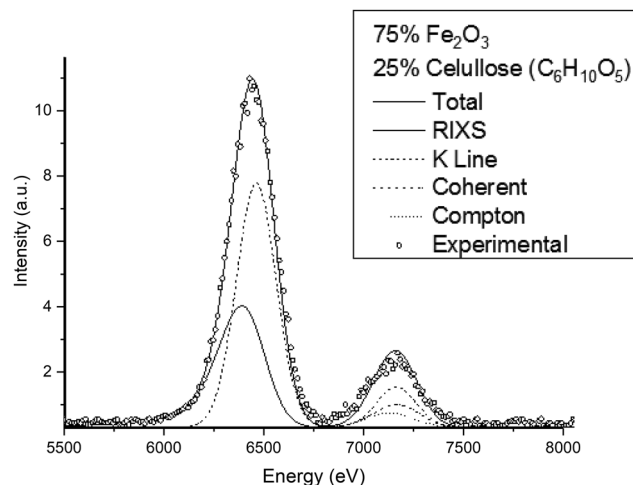


FIG. 3. Theoretical calculations of the different contributions to the emission of a  $\text{Fe}_2\text{O}_3$  sample (in cellulose). Dots indicates the measured data.

The energy distribution of the incident beam was represented as a set of Gaussian functions corresponding to the main reflection of the monochromator ( $E_0$ ), the first harmonic of the Si(111) crystal ( $3 \times E_0$ ), and the elastic scattering on the reflector of the characteristic lines of the Mo x-ray tube (Mo-K $\alpha$  and Mo-K $\beta$  lines). The relative intensities of these functions were 0.957, 0.009, 0.024, and 0.01, respectively. These values were obtained by direct measurements of the beam at the exit of the monochromator, corrected by detector efficiency.

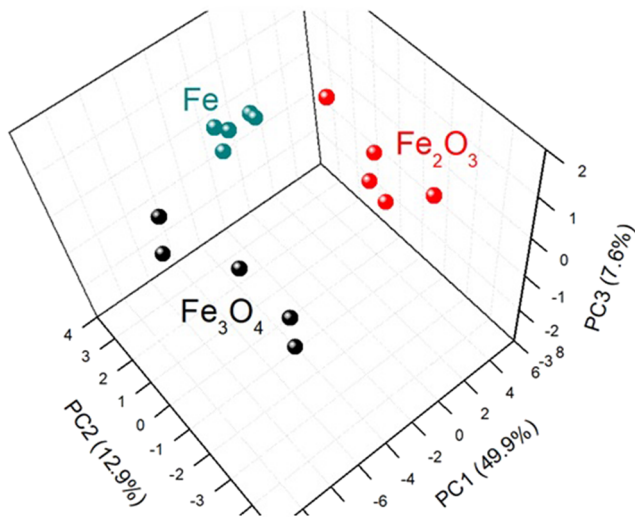
The final shape of the calculated peaks was obtained by convolution with the detector function. The real parameters of the XR100T detector were used, considering a resolution of 180 eV for the Mn-K $\alpha$  line. The geometry used was the same as the experimental setup described in Fig. 1. The solid angle of acceptance of the detector was set as  $10^{-5}$ .

A sample of 75% of  $\text{Fe}_3\text{O}_4$  + 25% of cellulose ( $\text{C}_6\text{H}_{10}\text{O}_5$ ) was studied in order to be compared with the experimental spectrum. Figure 3 shows the calculated intensities of the different components of the emitted spectrum from the sample (a linear background was subtracted). Open dots represent the experimental data obtained from the measurement under the conditions described in the previous subsection II C. As can be observed in Fig. 3, there is an excellent agreement with the calculations. The most important information of Fig. 3 lies in the [5.8–6.3] keV energy range. In this range, the low energy tail of the RIXS peak is the most important contribution to the spectrum, thus showing a good potential to discriminate the chemical environment of the samples.

### III. RESULTS AND DISCUSSION

Figure 4 shows, in the space defined by PC1, PC2, and PC3, the result of the PCA procedure to the set of RIXS spectra belonging to the three studied samples.





**FIG. 4.** Result of the PCA procedure to the measured Fe compounds. Analysis using Principal Components 1–3. The corresponding variability embraced by each PC is also indicated.

As it can be seen, and even when the number of acquired spectra is not so high, the different sets of measurement create well-defined 3D regions in this PC space, involving, each of them, the spectra belonging to a particular iron compound.

It is worth noting that the variability explained in this 3D space embraces 70.4% of the total variability of the system. This outcome highlights the fact that the internal structure of the RIXS peaks changed depending on the different chemical environments of the absorbing atom, in this case, iron.

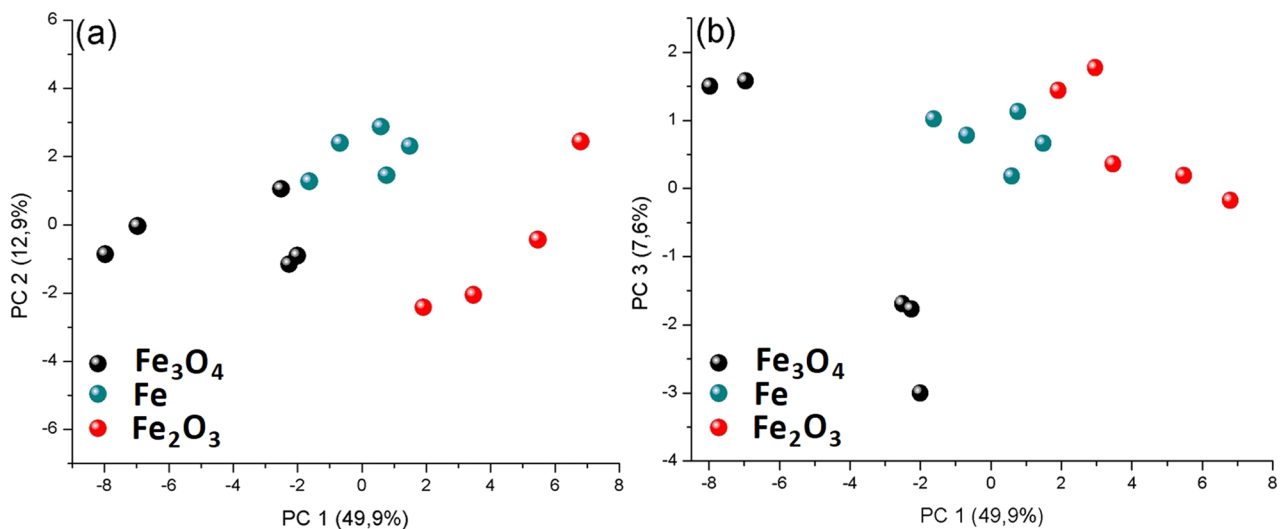
Figure 5 shows projections of the PCA result space on two particular planes: PC1–PC2 [Fig. 5(a)] and PC1–PC3 [Fig. 5(b)]. As it can be seen from both of them, for PC1 values below  $-2$ , this axis shows only the spectra belonging to a particular compound (Fe<sub>3</sub>O<sub>4</sub>). For values from  $-2$  to  $2$ , PC1 contains exclusively the information regarding the pure Fe sample. For values above  $\sim 2$ , PC1 exhibits only the spectra belonging to the Fe<sub>2</sub>O<sub>3</sub> oxide. This fact points out that the information explained by PC 1 is more than enough for a proper discrimination of all of the studied iron compounds, being then the analysis of this single axis sufficient for the proposed task. It should be remarked that this behavior is not surprising, since PC1 embraces almost 50% of the total variability explained by the studied system.

As can be appreciated from the data, the fine structure of the RIXS peaks allows the differentiation between the different studied iron compounds. In addition, the advantages of an energy dispersive system, such as user-friendly utilization, fast acquisition, and low cost, are also exploited.

The utilization of multivariate methods for the data analysis, in this case a simple PCA procedure, allowed a quick, straightforward, and reliable interpretation of the measurements, avoiding complicated and time demanding data analysis, such as deconvolution processes.

Since this work shows the first results of this EDIXS tool with an x-ray tube, it is possibly too soon for discussing the advantages of the proposed methodology. Nevertheless, it presents already clear advantages compared with conventional x-ray techniques (such as absorption ones), such as a fast acquisition, a low self-absorption, and, importantly, the absence of energy scans during the experiments.

Due to the flexibility of this tool, EDIXS offers the opportunity of investigating electron density changes in a variety of samples of interest applying diverse experimental geometries and setups, such as total reflection, grazing incident, and even confocal, for 3D studies. The EDIXS tool opens up the possibility of developing new



**FIG. 5.** Projections of the PCA results (Fig. 4) on the PC1–PC2 (a) and PC1–PC3 (b) planes. The corresponding variability embraced by each PC is also indicated.

methodologies for chemical speciation in conventional x-ray labs with multiple applications in several fields. Certainly, they cannot replace similar methodologies implemented in synchrotron or Free Electron Laser (FEL) facilities but complement the studies providing a very reliable first approximation of chemical state analysis by x-ray techniques. The potential of the technique is being confirmed by applications of the present spectrometer in environmental and health research with interesting preliminary results, which will be published in brief.

#### IV. CONCLUSIONS

Even when a simple setup was employed, the PCA procedure revealed that the fine structure of each RIXS peak clearly depends on the studied iron compound. These first results open the possibility of chemical state discriminations and characterizations by means of EDIXS using a conventional x-ray tube. This novel EDIXS tool would offer a unique opportunity to study chemical states of elements of interest in different kinds of samples, and even geometries, at a local x-ray tube based laboratory.

The next step consists of the improvement of the experimental setup, as a new monochromator, for the ulterior study of a variety of samples of interest by using the presented EDIXS methodology.

#### ACKNOWLEDGMENTS

This study was financed by SECyT-UNC (Grant No. 33620180100347CB) and by CONICET.

#### DATA AVAILABILITY

The data that support the findings of this study are available from the corresponding author upon reasonable request.

#### REFERENCES

- <sup>1</sup>J. J. Leani, J. I. Robledo, and H. J. Sánchez, *Spectrochim. Acta, Part B* **154**, 10 (2019).
- <sup>2</sup>C. J. Sparks, Jr., *Phys. Rev. Lett.* **33**, 262 (1974).
- <sup>3</sup>P. Eisenberger, P. M. Platzman, and H. Winick, *Phys. Rev. B* **13**, 2377 (1976).
- <sup>4</sup>P. Eisenberger, P. M. Platzman, and H. Winick, *Phys. Rev. Lett.* **36**, 623 (1976).
- <sup>5</sup>J. Tulkki and T. Aberg, *J. Phys. B: At., Mol. Phys.* **15**, L435 (1982).
- <sup>6</sup>W. Schülke, *J. Phys.: Condens. Matter* **13**, 7557–7591 (2001).
- <sup>7</sup>A. Kotani and S. Shin, *Rev. Mod. Phys.* **73**, 203 (2001).
- <sup>8</sup>K. Hämäläinen and S. Manninen, *J. Phys.: Condens. Matter* **13**, 7539 (2001).
- <sup>9</sup>P. Glatzel and U. Bergmann, *Coord. Chem. Rev.* **249**, 65 (2005).
- <sup>10</sup>J. J. Leani, H. J. Sánchez, M. C. Valentinuzzi, and C. Pérez, *J. Anal. Spectrom.* **26**, 378 (2011).
- <sup>11</sup>J. J. Leani, H. J. Sánchez, M. C. Valentinuzzi, and C. Pérez, *X-Ray Spectrom.* **40**, 254 (2011).
- <sup>12</sup>J. J. Leani, H. J. Sánchez, M. C. Valentinuzzi, C. Pérez, and M. C. Grenón, *J. Microsc.* **250**, 111 (2013).
- <sup>13</sup>J. I. Robledo, J. J. Leani, A. G. Karydas, A. Migliori, C. A. Pérez, and H. J. Sánchez, *Anal. Chem.* **90**, 3886 (2018).
- <sup>14</sup>H. J. Sánchez, J. J. Leani, C. A. Pérez, and R. D. Pérez, *J. Appl. Spectrosc.* **80**, 912 (2014).
- <sup>15</sup>J. I. Robledo, H. J. Sánchez, J. J. Leani, and C. A. Pérez, *Anal. Chem.* **87**, 3639 (2015).
- <sup>16</sup>J. J. Leani, H. J. Sánchez, and C. A. Pérez, *J. Spectrosc.* **2015**, 618279.
- <sup>17</sup>J. J. Leani, H. J. Sánchez, R. D. Pérez, and C. Pérez, *Anal. Chem.* **85**, 7069 (2013).
- <sup>18</sup>J. J. Leani, R. D. Pérez, J. I. Robledo, and H. J. Sánchez, *J. Anal. Spectrom.* **32**, 402 (2017).
- <sup>19</sup>D. Sokaras, T.-C. Weng, D. Nordlund, R. Alonso-Mori, P. Velikov, D. Wenger, A. Garachtchenko, M. George, V. Borzenets, B. Johnson, T. Rabedeau, and U. Bergmann, *Rev. Sci. Instrum.* **84**, 053102 (2013).
- <sup>20</sup>G. T. Seidler, D. R. Mortensen, A. J. Remesnik, J. I. Pacold, N. A. Ball, N. Barry, M. Styczinski, and O. R. Hoidn, *Rev. Sci. Instrum.* **85**, 113906 (2014).
- <sup>21</sup>H. J. Sánchez, *Nucl. Instrum. Methods, Sect. B* **194**, 90 (2002).
- <sup>22</sup>R. A. Johnson and D. W. Wichern, *Applied Multivariate Statistical Analysis*, 3rd ed. (Prentice-Hall, New Jersey, 1992).
- <sup>23</sup>K. H. Angeyo, S. Gari, J. M. Mangala, and A. O. Mustapha, *X-Ray Spectrom.* **41**(5), 321–327 (2012).
- <sup>24</sup>R. Fritzsche, P. M. Donaldson, G. M. Greetham, M. Towrie, A. W. Parker, and M. J. Baker, *Anal. Chem.* **90**(4), 2732–2740 (2018).
- <sup>25</sup>T. Shiraiwa and N. Fujino, *Jpn. J. Appl. Phys., Part 1* **5**, 886 (1966).
- <sup>26</sup>W. Schülke, “Inelastic scattering by electronic excitations,” in *Handbook on Synchrotron Radiation*, edited by G. Brown and D. E. Moncton (Elsevier, Amsterdam, 1991), Vol. 3, pp. 565–637.
- <sup>27</sup>H. J. Sanchez, M. C. Valentinuzzi, and J. J. Leani, *J. Anal. At. Spectrom.* **27**, 232 (2012).